Semiconductor Nanoplatelet Excimers

Benjamin T. Diroll,[†] Wooje Cho,[‡] Igor Coropceanu,[‡] Samantha M. Harvey,[§,∥]
Alexandra Brumberg,[§] Nicholas Holtgrewe,[⊥] Scott A. Crooker,[#] Michael R. Wasielewski,[§,∥]
Vitali B. Prakapenka,[⊥] Dmitri V. Talapin,[‡] and Richard D. Schaller*,[†,§,∥]

[†]Center for Nanoscale Materials, Argonne National Laboratory, Lemont, Illinois 60439, United States
[‡]Department of Chemistry, University of Chicago, Chicago, Illinois 60637, United States
[§]Department of Chemistry, Northwestern University, Evanston, Illinois 60208, United States
[∥]Institute for Sustainability and Energy, Northwestern University, Evanston, Illinois 60208, United States
[⊥]Center for Advanced Radiation Sources, University of Chicago, Chicago, Illinois 60439, United States
[#]National High Magnetic Field Laboratory, Los Alamos, New Mexico 87545, United States

ⓢ *Supporting Information*

ABSTRACT: Excimers, a portmanteau of "excited dimer", are transient species
that are formed from the electronic interaction of a fluorophore in the excited state
with a neighbor in the ground state, which have found extensive use as laser gain
media. Although common in molecular fluorophores, this work presents evidence
for the formation of excimers in a new class of materials: atomically precise two-
dimensional semiconductor nanoplatelets. Colloidal nanoplatelets of CdSe display
two-color photoluminescence resolved at low temperatures with one band
attributed to band-edge fluorescence and a second, red band attributed to excimer
fluorescence. Previously reasonable explanations for two-color fluorescence, such
as charging, are shown to be inconsistent with additional evidence. As with
excimers in other materials systems, excimer emission is increased by increasing
nanoplatelet concentration and the degree of cofacial stacking. Consistent with
their promise as low-threshold gain media, amplified spontaneous emission
emerges from the excimer emission line.

KEYWORDS: *Excimer, nanoplatelet, two-dimensional, photoluminescence, amplified spontaneous emission*
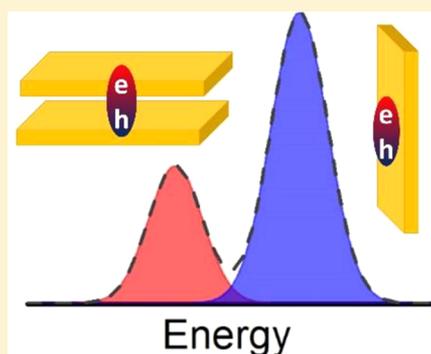
Colloidal nanoplatelets (NPLs) are two-dimensional
materials with an atomically precise thickness that
dominates quantum confinement.[1] These materials elicit
great interest for light-emitting applications[2−4] and have
demonstrated promise as laser gain media.[5−10] Strong van
der Waals interactions drive a propensity to form cofacial
assemblies that exhibit strong inter-NPL interactions, such as
fast Förster resonant energy transfer (FRET).[11−15] Excimer
("excited dimer") formation is a process related to FRET in
which a delocalized excited state is formed from an excited
fluorophore and a unexcited neighbor, evidenced by red-
shifted emission with no corresponding absorption feature.[16,17]
Although common in aromatic organic crystals,[18] which also
present homogeneous electronic structure and cofacial align-
ment, such emergent electronic structure has not been
identified in colloidal semiconductor nanocrystals, although
small metallic clusters are reported to form excimers[19,20] and
two-dimensional materials are known to from charge-separated
"interlayer excitons".[21] Here, we describe wide-ranging
measurements for CdSe NPLs that support an excimer-like
state which, further, yields amplified spontaneous emission
(ASE) from the excimeric photoluminescence (PL) band.

Photoemission from CdSe NPL ensembles at temperatures
below 100 K is known to consist of two closely spaced bands,
here termed "blue" and "red" for high- and low-energy features,
respectively. Several different explanations for this multistate
PL exist in the literature, including band-edge and phonon line
emission,[22,23] band-edge and trion emission,[24] or *s*- and excited
p-state exciton emission.[25] In this work, we revisit earlier
findings and present new experimental data that contradicts
these otherwise reasonable prior interpretations. Instead, data
on PL dynamics, polarization, and sensitivity to microstructure
support an explanation of two-state emission in which blue
emission arises from the band-edge *s* exciton state, while the
red emission arises from an excimer-like state emergent from
the collective electronic structure of neighboring NPLs. In
particular, the red PL feature shows strong sensitivity to
pressure, NPL concentration, and self-assembly into cofacial
stacks which is emblematic of excimer emission in molecular
fluorophores.[16,17]

The absorptions and PL of 3, 4, 5, and 6 monolayer (ML) NPL films are shown at both room temperature and 3 K in Figure 1a,b. Below 100 K, two features appear in the PL
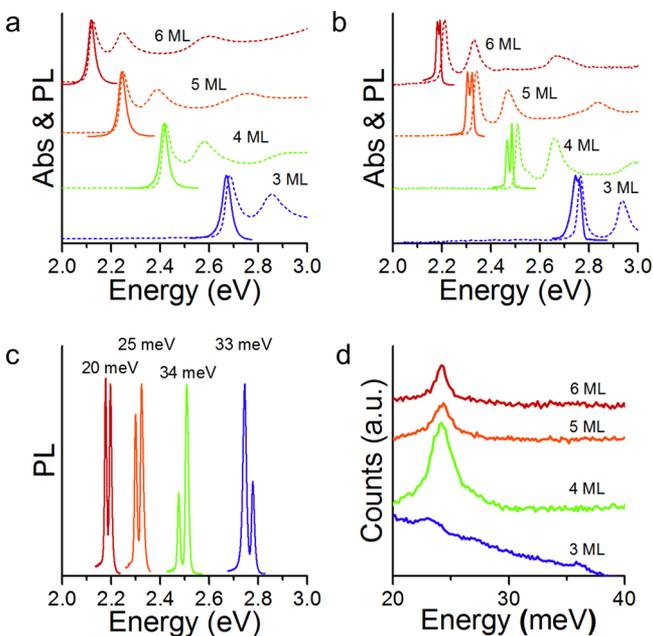

Figure 1. (a) Room temperature absorption (dashed lines) and PL (solid lines) of 3, 4, 5, and 6 ML CdSe NPLs prepared as solid drop-cast films. (b) Corresponding absorption and PL of the same samples collected at 3 K. (c) PL from frozen solutions of 3, 4, 5, and 6 ML CdSe NPLs at 80 K. (d) Raman spectra from the same samples as in (c). Raman spectra were collected with 479 nm light above the band gap for 4, 5, and 6 ML NPLs but not 3 ML NPLs.

spectrum of NPLs,[22,23,25] but the band-edge absorption feature remains a single resonance that is higher in energy than both PL features. Initially, the energy spacing of the PL features,

close to 25 meV, led to an assignment of the red PL as an LO phonon peak owing to very similar energy (25.4 meV).[22,23] Yet more recent work shows the energy spacings between the PL features depend on the NPL thickness[24] (as shown in Figure 1c) and lateral dimensions.[25] Effectively ruling out an LO phonon origin of the red PL feature, the energy spacing of the features varies from 20 to 34 meV in Figure 1c, compared to the 22−25 meV longitudinal optical (LO) phonon energies from Raman measurements presented in Figure 1d for the same samples. We also note that the energy spacings observed here are larger than previously identified negative trion emission in quantum wells[26,27] or trion emission features in epitaxial CdSe quantum dots at cryogenic temperatures.[28]

Earlier reports assign the two emission bands as band-edge and charged particle (trion)[24] emission or radiative recombination from s- and p-exciton states,[25] respectively. The blue PL feature becomes circularly polarized in a magnetic field, magnetically sensitive (Figure 2a), and close in energy to the absorption, whereas the red PL feature is magnetic field insensitive.[24] Upon the basis of these findings and the small Stokes shift of the blue PL, Shornikova et al. assigned the blue PL feature to band-edge emission and the red PL feature to strong trion emission.[24] Low-temperature PL measurements of NPLs embedded in uniaxially-stretched polymer films shown in Figure 2b demonstrate that the red PL feature is linearly polarized. (The elliptical projection of in-plane blue PL is also observed.) Although not conclusive, a similar phenomenon is observed in pyrene liquid crystals, in which the monomer fluorescence is polarized perpendicular to the liquid crystal director whereas excimer emission is polarized parallel to the director.[29]

To directly probe whether NPL trions give rise to the red emission, solutions of NPLs were treated with controlled amounts of either cobaltocene, an electron donor, or ferrocinium, an electron acceptor. At both ambient and cryogenic temperatures, mixing NPLs with cobaltocene
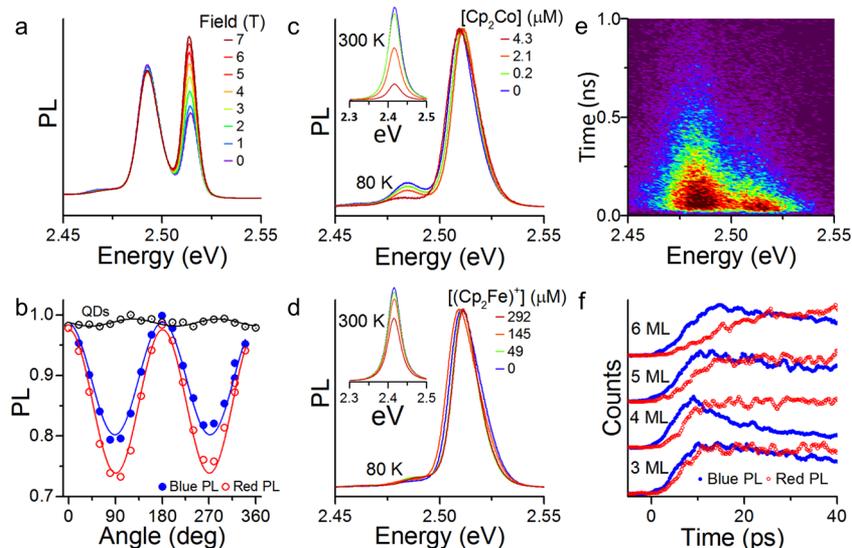

Figure 2. (a) Magnetic field dependence of PL from a sample of 4 ML CdSe NPLs at 4 K. (b) Emission polarization-dependent PL from the blue and red PL features of a 4 ML NPL in a stretched polymer film at 80 K. Unpolarized quantum dots (QDs) show the residual instrumental polarization. (c) PL of 4 ML frozen NPL solutions at 80 K in toluene with specified amounts of cobaltocene [Cp_2Co], normalized to the blue PL feature with un-normalized 300 K data inset. (d) PL of 4 ML frozen NPL solutions at 80 K in toluene with specified amounts of ferricinium hexafluorophosphate [$(Cp_2Fe)(PF_6)$], normalized to the blue PL feature, with un-normalized 300 K data inset. (e) Time- and energy-resolved PL from a solid film of 4 ML NPLs at 3 K. (f) Time-resolved PL at early times of red and blue PL features from solid film of NPLs collected at 3 K.

resulted in PL quenching, shown in Figure 2c, which suggests that negatively charged NPL trions show weaker PL than uncharged NPLs. With increasing cobaltocene concentration, the fraction of red PL actually decreased slightly, possibly due to competing nonradiative decay pathways. Ferricinium, as shown in Figure 2d, is a less potent quencher of PL and had no systematic effect on PL features.

PL dynamics shown in Figure 2e,f also present a challenge to explaining the red PL feature as a trion. The rise time of blue PL is close to the instrumental resolution but the red PL feature rises notably slower than the blue PL feature, increasing with NPL thickness (Figure 2f). The fitted exponential rise times for the sampled spots of the red PL are 4.9, 5.8, 7.6, and 18.3 ps for the 3, 4, 5, and 6 ML, respectively. Earlier works have also shown population transfer from the state responsible for blue PL to the state responsible for red PL[25] but trion formation is expected to be instantaneous[28] upon photon absorption by a NPL containing an extra charge. Previous reports of trion emission in electrochemically charged II−VI nanocrystals[30] have shown trion lifetimes shorter than uncharged exciton lifetimes in contrast to the longer red decay features shown in Supporting Information Figure S3 and multiple literature reports.[24,25] However, there remains ambiguity as trion lifetimes in epitaxial CdSe quantum dots are reported to be comparable or slightly longer than exciton lifetimes.[28] Neither case shows population transfer to the trion state emission. This population transfer has given rise to a hypothesis from Achtstein et al. of multistate emission in NPLs where the blue PL feature arises from an *p*-state exciton due to an LO phonon bottleneck that slows relaxation into the lowest excited *s*-state, accounting for the red PL.[25] However, the assignment of these features to *s*- and *p*-state emission is at odds with the absorption spectra (Figure 1b): both PL features are red-shifted from the first excitonic absorption feature for all samples. Additionally, measurements below demonstrate that the ratio of red and blue PL is not intrinsic to a given sample, but instead varies in a controllable manner.

Excimer-like emission as the origin of the red-shifted emission is consistent with data on the polarization properties of the samples and temporal dynamics that show population transfer from an optically active transition to a second transition with no absorption oscillator strength. As excimers are highly sensitive to concentration and orientation, evidence that microstructure plays an important role in dictating the proportions and energetic spacing of the red and blue PL features is also consistent with an inter-NPL origin of the red PL feature. Even in early reports, the occurrence of one or two PL features from NPL solids was noted as contingent on the microstructure.[22] Consistent with this finding, the intensity of the red and blue PL is variable on a submillimeter length-scale across film samples produced by drop-casting, demonstrated with a spatial PL map of a 4 ML NPL film in Figure 3a. Frozen solutions of NPLs yield a ratio of PL intensity which is more reproducible by comparison, suggesting that local structure plays an important role in NPL PL.

Cryogenic, pressure-dependent optical studies of NPL films, which bring NPLs closer together at higher pressure,[31] are also consistent with inter-NPL origin of red PL. Below 1 GPa, NPL excitonic structure and PL are preserved but blue-shifted from the ambient pressure conditions (Figure 3b).[32] In earlier measurements, pressures of approximately 1 GPa reduced edge-to-edge spacing of oleate-capped nanocrystals by 3.5 Å, primarily by compressing the surface ligands.[31] NPLs show
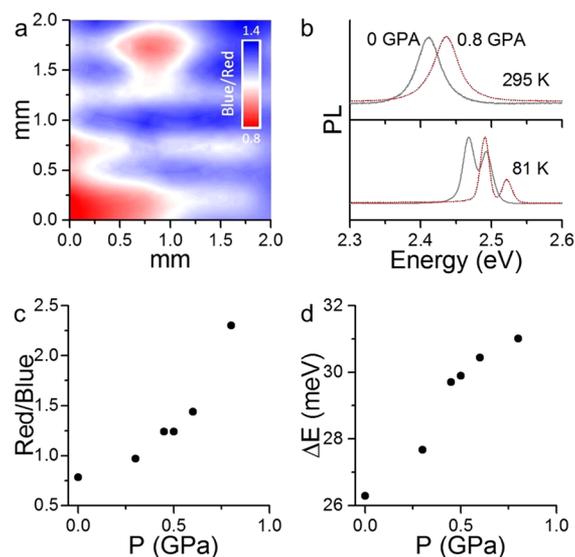

Figure 3. (a) PL map of 4 mm^2 area of drop-cast film of 4 ML NPLs showing variation in the red and blue PL intensities. (b) PL spectra of 4 ML CdSe NPLs under hydrostatic pressure in an ethanol-methanol medium at 295 and 81 K. (c) Ratio of integrated red PL feature compared to the integrated blue PL feature as a function of pressure at 81 K. To ensure comparability of the PL data in light of (a), the full field of the exposed diamond was illuminated. (d) Energetic spacing of red and blue PL features of a 4 ML CdSe NPL film at 81 K as a function of pressure.

edge-to-edge spacings at ambient pressure of 40 Å (Supporting Information Figure S4), which is reduced at modest pressures. At these increased pressures, the ratio of red PL increases compared to the blue PL, indicating that closer proximity facilitates the red PL and suggesting that the PL originates from an emergent state of multiple NPLs which may more readily spread over multiple NPLs.[33] We note that pyrene aggregates under pressure also exhibit increasing excimer emission with pressure,[34] although the relative intensities of excimer and monomer emission reflect complex changes in lifetime and morphology.[35,36] Also accompanying closer edge-to-edge spacing, the red and blue PL features of a drop-cast NPL solid show increasing energetic spacing with pressure (Figure 3d). Compared to ambient conditions, the spacing increased by approximately 20% at 0.8 GPa for the same NPL sample, another indication of structurally modulated electronic structure. The increasing spacing of the two PL features in energy is attributed to increased coupling of neighboring NPLs, lowering the energy of the red PL with respect to the blue PL, which retains a similar Stokes shift compared to the absorption.[32]

The strength of excimer emission should increase with fluorophore concentration.[16,37] Figure 4b−e shows PL spectra from frozen NPL solutions in methylcyclohexane for a series of NPL concentrations. For all samples, at higher NPL concentrations, the red PL feature increases in intensity relative to the blue PL feature, a phenomenon which is classically associated with excimer formation.[17] To study the influence of NPL orientation, which may also have a substantial role in both FRET and excimer formation,[11,14,15,38] dilute NPL solutions were measured with varying amounts of ethanol, an antisolvent which induces cofacial NPL stacking.[14] As shown in Figure 4e−i, with ethanol addition and NPL stack formation the red PL feature increases in relative intensity for
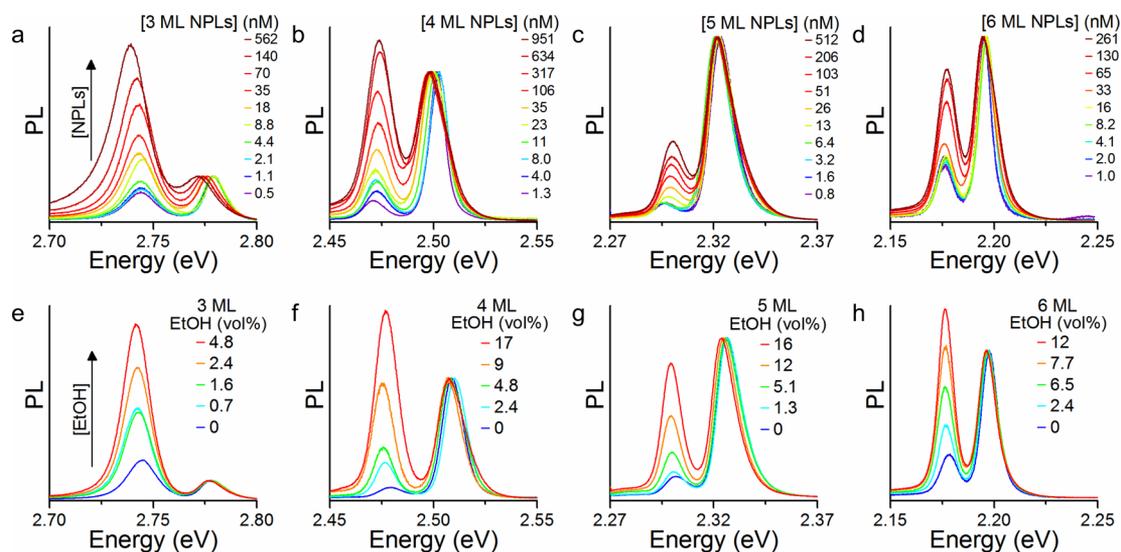
Figure 4. (a−d) Normalized PL from frozen methylcyclohexane solutions of CdSe NPLs at varying concentrations. Concentration values are estimated from absorption spectra based upon reported extinction. (e−h) Normalized PL collected from rapidly frozen methylcyclohexane solutions of CdSe NPLs at 80 K with the labeled volume fraction of ethanol.

Scheme 1. Partial Scheme of Excited States of Colloidal NPLs[a]
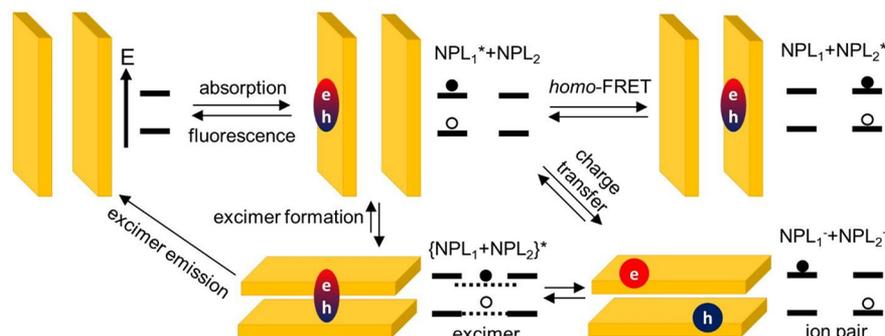
[a]Non-specific trapping and non-radiative recombination pathways are not included. Although there is no arrow, recombination of the ion pair state is also conceivable.

frozen solutions of all thicknesses of NPLs. This implicates the formation of NPL stacks in particular as key to enhancement of the red excimer PL feature. In addition, it is unclear how such an observable may be reconciled with pictures of charged (trion) NPL emission or dual s- and p-state PL.

It is noteworthy, however, that two PL features appear in all of the spectra in Figure 4. Incomplete suppression of the red PL feature presents a challenge to any explanations, like that of an excimer, in which inter-NPL interactions leads to the red PL feature. However, experiments suggest that the persistence of the red PL feature at low concentrations and minimized aggregation arises from transient aggregates or intra-NPL interactions when NPLs form scroll-like structures.[39] Scroll-like structures permit an intra-NPL structure (and excimer) which closely resembles that of NPL stacks. An intra-NPL origin is particularly supported by a relative increase in the red PL for larger NPLs of the same thickness, which are more likely to form scroll structures (Supporting Information Figure S5).

Scheme 1 presents a coarse picture of NPL excimer formation in competition with homo-FRET, fluorescence, and charge transfer, which is another possibility not explicitly raised in the literature that is considered here. All of these

states may occur within the same sample without precluding the others. Indeed, in many molecular systems, both direct and ion-pair-mediated conversion between monomers and excimers are known.[40−42] FRET, charge transfer, and excimer formation are all more likely at higher NPL densities, which can be achieved with concentration or purposeful aggregation. For most of the measurements presented here, homo-FRET is optically passive because the PL of the donor and acceptor are identical, although this process may reduce quantum yield or adjust apparent lifetime.[11,14] A few factors and observables favor an excimer-like emission as opposed to spatially indirect emission from a charge transfer ion pair. First, the NPLs are isoenergetic and therefore have no static driving force for charge transfer; this distinguishes them from "interlayer excitons" as known in two-dimensional materials, which occur due to band offsets in a type-II alignment.[21] Second, the spatially indirect exciton recombination lifetime of an ion pair should be much longer (10−100 times longer in semiconductor nanostructures) than the monomer.[43] Here, the red PL decay is longer than blue PL, but still subnanosecond; the small increase in lifetime is more similar to the factor of 3−5 increase in lifetime observed in excimers.[18,37] Additional evidence that the red PL does not
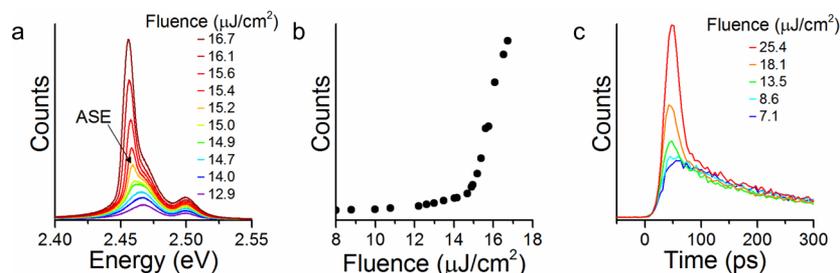
Figure 5. (a) Fluence-dependent emission from 340 μm spot of a solid film of 4 ML CdSe NPLs collected at 80 K. The ASE peak, which has a full-width at half-maximum of 7 meV (2.3 nm) is indicated on the plot. (b) Counts of 4 ML NPL film versus input fluence. The ASE threshold is estimated as 14.8 μJ/cm². (c) Early time fluence-dependent dynamics from a different sample spot of a solid film of 4 ML CdSe NPLs at 80 K.

originate from a charge transfer state comes from the low-temperature emission of CdSe/CdS core/shell NPLs, which *do* display at least partial charge-separated character and substantially longer emission (Supporting Information Figure S6).

Taken together, dynamic and time-integrated data is consistent with an excimer-like emission to explain the red PL feature that is observed at low temperatures. Evidence from other literature also supports assignment of red PL to excimer emission. Reported single-NPL emission at 20 K contains no second PL feature.[44] Room-temperature Stark effect measurements of NPL ensembles also show two components of PL, which may be resolved with large electric fields.[45] Unlike homo-FRET, excimer emission is always red-shifted from monomer PL, as is observed here.[17] Although in organic fluorophores excimer emission is usually broad,[17] we note that NPLs have less configurational entropy and smaller electron–phonon coupling.

One of the most important technological contributions of excimers is to excimer (or exciplex) lasers. The red-shifted transitions of such excitations reduce loss associated with reabsorption for normal Stokes-shifted emission and generate a third level in the optical system which facilitates gain. NPLs are already recognized for low optical pumping thresholds of ASE and lasing.[5−9] Fluence-dependent measurements of drop-cast 4 ML NPLs at 80 K in Figure 5a show the growth of an additional emission feature of narrower bandwidth (7 meV or 2.3 nm full-width at half-maximum) at higher excitation fluence arising from ASE on the red edge of the excimer feature. The ASE threshold, determined from the onset of superlinear emission in Figure 5b, is 14.8 μJ/cm², comparable to reported room-temperature values.[6] Dynamics measurements in Figure 5c show that the new spectral feature is accompanied by a new ultrafast ASE emission feature. These results strongly indicate that NPLs can be exploited as excimer lasers and also suggest excimer formation represents another underlying rationale for observed low-threshold or CW lasing at room temperature.

In conclusion, our measurements indicate that multistate emission from CdSe NPLs, which is resolved at low temperature, depends strongly on microstructure and concentration consistent with excimer-like emission. In particular, the red PL feature has a relative intensity which increases with NPL concentration and aggregation into stacked structures, changes in energy dependent on inter-NPL spacing, and does not present oscillator strength in absorption. This phenomenon most likely occurs due to the isoenergetic electronic structure of the NPLs and their propensity to form cofacial stacks, traits which distinguish the NPLs from other nano-

crystal systems, but which are common for two-dimensional materials such as van der Waals heterostructures. Although the multiple emissive states in these samples are only spectrally resolved at low temperatures, they may also be expected under ambient conditions. These results suggest that controlling the morphology of atomically precise two-dimensional material assemblies can result in emergent electronic structure (compatible with concepts of mini-bands) that is not achieved in isolated two-dimensional materials or related bulk analogues, and furthermore, that this emergent electronic structure can both facilitate exploitation and present local excitation traps in optoelectronic devices.

■ ASSOCIATED CONTENT

ⓢ Supporting Information

The Supporting Information is available free of charge on the ACS Publications website at DOI: 10.1021/acs.nanolett.8b02865.

> Experimental details and additional microscopy and optical data characterization (PDF)

■ AUTHOR INFORMATION

Corresponding Author
*E-mail: schaller@anl.gov.

ORCID ⓞ
Benjamin T. Diroll: 0000-0003-3488-0213
Wooje Cho: 0000-0002-4022-4194
Alexandra Brumberg: 0000-0003-2512-4686
Scott A. Crooker: 0000-0001-7553-4718
Michael R. Wasielewski: 0000-0003-2920-5440
Dmitri V. Talapin: 0000-0002-6414-8587
Richard D. Schaller: 0000-0001-9696-8830

Notes
The authors declare no competing financial interest.

■ ACKNOWLEDGMENTS

■ REFERENCES

(1) Ithurria, S.; Tessier, M. D.; Mahler, B.; Lobo, R. P. S. M.; Dubertret, B.; Efros, A. L. *Nat. Mater.* **2011**, *10* (12), 936−941.

(2) Cunningham, P. D.; Souza, J. B.; Fedin, I.; She, C.; Lee, B.; Talapin, D. V. *ACS Nano* **2016**, *10* (6), 5769−5781.

(3) Chen, Z.; Nadal, B.; Mahler, B.; Aubin, H.; Dubertret, B. *Adv. Funct. Mater.* **2014**, *24* (3), 295−302.

(4) Giovanella, U.; Pasini, M.; Lorenzon, M.; Galeotti, F.; Lucchi, C.; Meinardi, F.; Luzzati, S.; Dubertret, B.; Brovelli, S. *Nano Lett.* **2018**, *18* (6), 3441−3448.

(5) She, C.; Fedin, I.; Dolzhnikov, D. S.; Demortière, A.; Schaller, R. D.; Pelton, M.; Talapin, D. V. *Nano Lett.* **2014**, *14* (5), 2772−2777.

(6) She, C.; Fedin, I.; Dolzhnikov, D. S.; Dahlberg, P. D.; Engel, G. S.; Schaller, R. D.; Talapin, D. V. *ACS Nano* **2015**, *9* (10), 9475−9485.

(7) Diroll, B. T. B. T.; Talapin, D. V. D. V.; Schaller, R. D. R. D. *ACS Photonics* **2017**, *4* (3), 576−583.

(8) Yang, Z.; Pelton, M.; Fedin, I.; Talapin, D. V.; Waks, E. *Nat. Commun.* **2017**, *8* (1), 143.

(9) Grim, J. Q.; Christodoulou, S.; Di Stasio, F.; Krahne, R.; Cingolani, R.; Manna, L.; Moreels, I. *Nat. Nanotechnol.* **2014**, *9* (11), 891−895.

(10) Olutas, M.; Guzelturk, B.; Kelestemur, Y.; Yeltik, A.; Delikanli, S.; Demir, H. V. *ACS Nano* **2015**, *9* (5), 5041−5050.

(11) Guzelturk, B.; Olutas, M.; Delikanli, S.; Kelestemur, Y.; Erdem, O.; Demir, H. V. *Nanoscale* **2015**, *7* (6), 2545−2551.

(12) Erdem, O.; Olutas, M.; Guzelturk, B.; Kelestemur, Y.; Demir, H. V. *J. Phys. Chem. Lett.* **2016**, *7* (3), 548−554.

(13) Jana, S.; Phan, T. N. T.; Bouet, C.; Tessier, M. D.; Davidson, P.; Dubertret, B.; Abécassis, B. *Langmuir* **2015**, *31* (38), 10532−10539.

(14) Guzelturk, B.; Erdem, O.; Olutas, M.; Kelestemur, Y.; Demir, H. V. *ACS Nano* **2014**, *8* (12), 12524−12533.

(15) Rowland, C. E.; Fedin, I.; Zhang, H.; Gray, S. K.; Govorov, A. O.; Talapin, D. V.; Schaller, R. D. *Nat. Mater.* **2015**, *14* (5), 484.

(16) Förster, T.; Kasper, K. *Z. Phys. Chem.* **1954**, *1* (5-6), 275−277.

(17) Lakowicz, J. R. *Principles of Fluorescence Spectroscopy*, 3rd ed.; Lakowicz, J. R., Ed.; Springer US: Boston, MA, 2006.

(18) Cohen, M. D. *Mol. Cryst. Liq. Cryst.* **1979**, *50* (1), 1−10.

(19) Santiago-Gonzalez, B.; Monguzzi, A.; Azpiroz, J. M.; Prato, M.; Erratico, S.; Campione, M.; Lorenzi, R.; Pedrini, J.; Santambrogio, C.; Torrente, Y.; De Angelis, F.; Meinardi, F.; Brovelli, S. *Science* **2016**, *353* (6299), 571−575.

(20) Santiago-Gonzalez, B.; Monguzzi, A.; Capitani, C.; Prato, M.; Santambrogio, C.; Meinardi, F.; Brovelli, S. *Angew. Chem., Int. Ed.* **2018**, *57* (24), 7051−7055.

(21) Rivera, P.; Schaibley, J. R.; Jones, A. M.; Ross, J. S.; Wu, S.; Aivazian, G.; Klement, P.; Seyler, K.; Clark, G.; Ghimire, N. J.; Yan, J.; Mandrus, D. G.; Yao, W.; Xu, X. *Nat. Commun.* **2015**, *6*, 4−9.

(22) Tessier, M. D.; Biadala, L.; Bouet, C.; Ithurria, S.; Abecassis, B.; Dubertret, B. *ACS Nano* **2013**, *7* (4), 3332−3340.

(23) Biadala, L.; Liu, F.; Tessier, M. D.; Yakovlev, D. R.; Dubertret, B.; Bayer, M. *Nano Lett.* **2014**, *14* (3), 1134−1139.

(24) Shornikova, E. V.; Biadala, L.; Yakovlev, D. R.; Sapega, V. F.; Kusrayev, Y. G.; Mitioglu, A. A.; Ballottin, M. V.; Christianen, P. C. M.; Belykh, V. V.; Kochiev, M. V.; Sibeldin, N. N.; Golovatenko, A. A.; Rodina, A. V.; Gippius, N. A.; Kuntzmann, A.; Jiang, Y.; Nasilowski, M.; Dubertret, B.; Bayer, M. *Nanoscale* **2018**, *10* (2), 646−656.

(25) Achtstein, A. W.; Scott, R.; Kickhöfel, S.; Jagsch, S. T.; Christodoulou, S.; Bertrand, G. H. V.; Prudnikau, A. V.; Antanovich, A.; Artemyev, M.; Moreels, I.; Schliwa, A.; Woggon, U. *Phys. Rev. Lett.* **2016**, *116* (11), 116802.

(26) Sergeev, R. A.; Suris, R. A.; Astakhov, G. V.; Ossau, W.; Yakovlev, D. R. *Eur. Phys. J. B* **2005**, *47* (4), 541−547.

(27) Solovyev, V. V.; Kukushkin, I. V. *Phys. Rev. B: Condens. Matter Mater. Phys.* **2009**, *79* (23), 233306.

(28) Patton, B.; Langbein, W.; Woggon, U. *Phys. Rev. B: Condens. Matter Mater. Phys.* **2003**, *68* (12), 1−9.

(29) Stegemeyer, H.; Hasse, J.; Laarhoven, W. *Chem. Phys. Lett.* **1987**, *137* (6), 516−520.

(30) Jha, P. P.; Guyot-Sionnest, P. *ACS Nano* **2009**, *3* (4), 1011−1015.

(31) Podsiadlo, P.; Lee, B.; Prakapenka, V. B.; Krylova, G. V.; Schaller, R. D.; Demortière, A.; Shevchenko, E. V. *Nano Lett.* **2011**, *11* (2), 579−588.

(32) Zhou, B.; Xiao, G.; Yang, X.; Li, Q.; Wang, K.; Wang, Y. *Nanoscale* **2015**, *7* (19), 8835−8842.

(33) Bains, G. K.; Kim, S. H.; Sorin, E. J.; Narayanaswami, V. *Biochemistry* **2012**, *51* (31), 6207−6219.

(34) Johnson, P. C.; Offen, H. W. *J. Chem. Phys.* **1973**, *59*, 801−806.

(35) Johnson, P. C.; Offen, H. W. *J. Chem. Phys.* **1972**, *56* (4), 1638−1642.

(36) Kim, J. J.; Beardslee, R. A.; Phillips, D. T.; Offen, H. W. *J. Chem. Phys.* **1969**, *51* (6), 2761−2762.

(37) Förster, T. *Angew. Chem., Int. Ed. Engl.* **1969**, *8* (5), 333−343.

(38) Yoo, H.; Yang, J.; Yousef, A.; Wasielewski, M. R.; Kim, D. *J. Am. Chem. Soc.* **2010**, *132* (11), 3939−3944.

(39) Schlenskaya, N. N.; Yao, Y.; Mano, T.; Kuroda, T.; Garshev, A. V.; Kozlovskii, V. F.; Gaskov, A. M.; Vasiliev, R. B.; Sakoda, K. *Chem. Mater.* **2017**, *29* (2), 579−586.

(40) Cook, R. E.; Phelan, B. T.; Kamire, R. J.; Majewski, M. B.; Young, R. M.; Wasielewski, M. R. *J. Phys. Chem. A* **2017**, *121* (8), 1607−1615.

(41) Miller, C. E.; Wasielewski, M. R.; Schatz, G. C. *J. Phys. Chem. C* **2017**, *121* (19), 10345−10350.

(42) Wu, Y.; Zhou, J.; Phelan, B. T.; Mauck, C. M.; Stoddart, J. F.; Young, R. M.; Wasielewski, M. R. *J. Am. Chem. Soc.* **2017**, *139* (40), 14265−14276.

(43) Choi, C. L.; Li, H.; Olson, A. C. K.; Jain, P. K.; Sivasankar, S.; Alivisatos, a P. *Nano Lett.* **2011**, *11* (6), 2358−2362.

(44) Tessier, M. D.; Javaux, C.; Maksimovic, I.; Loriette, V.; Dubertret, B. *ACS Nano* **2012**, *6* (8), 6751−6758.

(45) Scott, R.; Achtstein, A. W.; Prudnikau, A. V.; Antanovich, A.; Siebbeles, L. D. A.; Artemyev, M.; Woggon, U. *Nano Lett.* **2016**, *16* (10), 6576−6583.